

---

# Physics-aware registration based auto-encoder for convection dominated PDEs

---

**Rambod Mojjani**

Department of Aerospace Engineering  
University of Illinois at Urbana-Champaign  
Urbana, IL 61801  
mojjani2@illinois.edu

**Maciej Balajewicz**

Department of Aerospace Engineering  
University of Illinois at Urbana-Champaign  
Urbana, IL 61801  
mbalajew@illinois.edu

## Abstract

We design a physics-aware auto-encoder to specifically reduce the dimensionality of solutions arising from convection-dominated nonlinear physical systems. Although existing nonlinear manifold learning methods seem to be compelling tools to reduce the dimensionality of data characterized by a large Kolmogorov  $n$ -width, they typically lack a straightforward mapping from the latent space to the high-dimensional physical space. Moreover, the realized latent variables are often hard to interpret. Therefore, many of these methods are often dismissed in the reduced order modeling of dynamical systems governed by the partial differential equations (PDEs). Accordingly, we propose an auto-encoder type nonlinear dimensionality reduction algorithm. The unsupervised learning problem trains a diffeomorphic spatio-temporal grid, that registers the output sequence of the PDEs on a non-uniform parameter/time-varying grid, such that the Kolmogorov  $n$ -width of the mapped data on the learned grid is minimized. We demonstrate the efficacy and interpretability of our approach to separate convection/advection from diffusion/scaling on various manufactured and physical systems.

## 1 Introduction

Many physical phenomena are modeled using partial differential equations (PDEs). High accuracy simulations of these large-scale nonlinear systems often require extensive computational resources. Although cheaper and faster processors, as well as highly parallel architectures, have made many of such large-scale computations viable, reduced order models of these systems remain attractive, especially in many-query simulations and real-time control.

The goal of reduced order modeling is to leverage the vast amount of data generated from high accuracy simulations to learn a low-dimensional model that can accurately and efficiently approximate the underlying dynamical system. This is especially a challenging task for convection dominated PDEs, where the Kolmogorov  $n$ -width of the snapshots of the solution is relatively large, i.e. the solution cannot be effectively reduced on a linear subspace. Such problems emerge frequently in a broad range of applications, from Navier-Stokes equations (fluid dynamics) to Schrödinger equation (quantum-mechanical systems) [1]. In the machine learning community, the recognition of similar challenge dates back to 1990s and attempts in classification of handwritten digits [2], where presence of simple transformations such as translations and rotations in the data-set is well known to dramatically deteriorate the accuracy of linear methods such as principle component analysis (PCA). Fundamentally, other linear manifolds (subspaces) suffer from similar drawbacks, examples include proper orthogonal decomposition (POD), multidimensional scaling (MDS) [3], factor analysis [4] and independent component analysis (ICA) [4]. Therefore, the high dimensionality of the data on any of these linear manifolds has incentivized a slew of nonlinear manifold learning approaches, such as Iso-map [5], kernel PCA [6], locally linear embedding (LLE) [7], Laplacian eigenmaps

(LEM) [8], semi-definite embedding (SDE) [9], auto-encoders [10], t-SNE [11], and diffeomorphic dimensionality reduction [12].

Although many of the aforementioned nonlinear methods provide the sought after low-dimensional manifold, only a few provide the mapping from the learned low-dimensional to the high-dimensional manifold, for a survey [see 13]. This is especially important in reduced order modeling of PDEs, since the models are to be evolved in the parameters space or time on the low-dimensional manifold, i.e. evolving of the latent variables, and subsequently the latent variables have to be mapped to the physical high-dimensional manifold. Auto-encoders (AE), specifically convolutional auto-encoders (CAEs) [14] and deep convolutional generative adversarial networks (DCGANs) [15], are amongst the successful methods used in dimensionality reduction of PDEs [13, 16]. However, linear manifolds such as proper orthogonal decomposition (POD) and dynamic mode decomposition (DMD) are still often extensively preferred to these nonlinear approaches, since they provide an interpretable framework for analysis of the system, as well as controlling of the reduced system. POD reveals the coherent structures in fluid flows [17, 18], and DMD obtains a finite-dimensional, matrix approximations of the Koopman operator, which opens the possibility of taking advantage of estimation and control theories developed for the linear systems [19]. In a more recent effort, it is shown that deep AE architectures can be trained to transform nonlinear PDEs into linear PDEs, by learning the eigen-function of the Koopman operator [20]. In this approach, although the transformation is nonlinear, the latent variables lie on a linear subspace. Finally, a similar approach that prioritizes the optimal reducibility by learning a nonlinear manifold leads to a low-dimensional latent space. Therefore, by definition, such an approach results in a more efficient reduced order model.

In this paper, we develop an AE to learn a manifold on which the reduced order models can be efficiently constructed. To this end, we pose an unsupervised learning problem, that learns a spatio-temporal grid on which the low-rank linear decomposition of the solution of the PDE is optimal. The method can be interpreted as learning a map that registers the output sequence of a convection-dominated PDE to a low-rank reconstruction of the solution. The method is in spirit of registration based manifold learning approaches, e.g. [12, 21]. Furthermore, we demonstrate the efficacy of our approach in reducing some inherently challenging problems. Finally, we discuss how the realized grid can be interpreted as a low-rank representation of information traveling in the domain and how it separates convection/advection from diffusion/scaling on the example problems.

## 2 Preliminaries

In approximation theory, Kolmogorov n-width is used to measure how well the data – the solution of the PDEs in the context of this paper– can be approximated on a linear manifold, i.e. subspace. The connection between the Kolmogorov n-width and POD of the data is rigorously established [22], leading to a measure on the accuracy and feasibility of a low-rank reduced order model on a subspace.

Constructing the bases from snapshots in the spirit of the POD method can be formulated as a low-rank matrix approximation problem as follows: For a given snapshot matrix  $\mathbf{M} \in \mathbb{R}^{N \times K}$ , find a low rank matrix  $\widetilde{\mathbf{M}} \in \mathbb{R}^{N \times K}$  that solves the minimization problem

$$\underset{\text{rank}(\widetilde{\mathbf{M}})=k}{\text{minimize}} \quad \left\| \mathbf{M} - \widetilde{\mathbf{M}} \right\|_F, \quad (1)$$

where for a successful reduction,  $k \ll N$  and  $k \ll K$ . A snapshot matrix is here a matrix whose columns contain the states of the system of interest. More specifically, each column corresponds to the state of the system for some particular value of the system parameters, time, or the boundary/initial conditions. Hence,  $\mathbf{M} = [\mathbf{w}_1, \dots, \mathbf{w}_K]$ , where  $\mathbf{w}_i \in \mathbb{R}^N$  is the state at the  $i^{\text{th}}$  parameter or time step.

In problem (1), the rank constraint can be taken care of by representing the unknown matrix as  $\widetilde{\mathbf{M}} = \mathbf{U}\mathbf{V}$ , where  $\mathbf{U} \in \mathbb{R}^{N \times k}$  and  $\mathbf{V} \in \mathbb{R}^{k \times K}$ , so that problem (1) becomes

$$\underset{\mathbf{U}, \mathbf{V}}{\text{minimize}} \quad \left\| \mathbf{M} - \mathbf{U}\mathbf{V} \right\|_F. \quad (2)$$

It is well known that the solution of the above low-rank approximation problem is given by the singular value decomposition (SVD) of  $\mathbf{M}$ . Specifically,  $\mathbf{U} = [\mathbf{u}_1, \dots, \mathbf{u}_k] \in \mathbb{R}^{N \times k}$  and  $\mathbf{V} =$

$\Sigma [\mathbf{v}_1, \dots, \mathbf{v}_k] \in \mathbb{R}^{k \times K}$ , where  $\mathbf{M} = \mathbf{U}^* \Sigma^* \mathbf{V}^{*T}$ ,  $\mathbf{U}^* = [\mathbf{u}_1, \dots, \mathbf{u}_k, \mathbf{u}_{k+1}, \dots, \mathbf{u}_N]$ ,  $\mathbf{V}^{*T} = [\mathbf{v}_1, \dots, \mathbf{v}_k, \mathbf{v}_{k+1}, \dots, \mathbf{v}_K]$ , and  $\Sigma^* = \text{diag}(\sigma_1, \sigma_2, \dots, \sigma_r)$  is a diagonal rank- $r$  matrix of singular values, where  $\sigma_1 \geq \sigma_2 \geq \dots \geq \sigma_r$ , and  $\Sigma = \text{diag}(\sigma_1, \sigma_2, \dots, \sigma_k)$ . This is called ‘‘method of snapshots’’ for computing the POD bases [23]. This decomposition has a very close connotation to factor analysis [4] and can be reproduced by artificial neural networks with linear activations [24]. Although the linearity of the learned manifold leads to inefficiencies in convection-dominated PDEs with large Kolmogorov n-width, the existence of a closed form solution as well as the abundance of computationally efficient approaches, such as [25], has made the method predominately be utilized in the field. Our goal is to extend the norm minimization problem of (2) to an interpretable and efficient nonlinear manifold learning problem.

### 3 Physics-aware registration

We generalize the linear manifold learning problem of (1), as a nonlinear manifold learning as follows: For a given data-set lying on the high-dimensional manifold, learn a manifold, and the corresponding mapping, on which the solution can be expressed as a low-rank linear decomposition. The map from the high-dimensional physical manifold to the learned manifold is denoted by  $\mathcal{G}$  and the inverse by  $\mathcal{G}^{-1}$ . In the finite-dimension matrix form where  $\mathcal{G} : \mathbb{R}^{N \times K} \rightarrow \mathbb{R}^{N \times K}$  and  $\mathcal{G}^{-1} : \mathbb{R}^{N \times K} \rightarrow \mathbb{R}^{N \times K}$ , the minimization problem has the following form:

$$\text{minimize} \quad \left\| \mathbf{M} - \mathcal{G}^{-1}(\widetilde{\mathbf{M}}) \right\|_F. \quad (3)$$

In this case,  $\widetilde{\mathbf{M}} = \mathbf{U}\mathbf{V}$  is the linear decomposition the data on the learned manifold, where  $\mathbf{U} \in \mathbb{R}^{N \times k_r}$  and  $\mathbf{V} \in \mathbb{R}^{k_r \times K}$ . In principle, the compression of the data on the learned manifold is lossless. For the compression to be successful  $k_r \ll N$  and  $k_r \ll K$ , and it outperforms (1) if and only if  $k_r < k$ .

In this formulation, both the high-dimensional snapshots and its low-dimensional representation on the learned manifold (latent variables) are stored in a matrix. In contrast to most machine vision tasks dealing with images, the data does not necessarily lie on a uniform Cartesian grid. This is important since many of the PDEs are discretized on unstructured computational grids, while many of the traditional machine learning tools are developed for uniform Cartesian grids representing an image. Often, the snapshot matrix of  $\mathbf{M}$  is defined on a constant grid (in physics: Eulerian framework) and  $\widetilde{\mathbf{M}}$ , by construct, is associated to the snapshots of latent variables on a parameter/time-varying grid (in physics: arbitrary Lagrangian Eulerian framework). Therefore, (3) can be interpreted as a registration task, that minimizes the Kolmogorov n-width of the snapshots of the latent variables on the learned parameter/time-varying grid.

#### 3.1 Diffeomorphism and interpolation

We impose diffeomorphism as a condition on the mapping to and from the learned manifold: By definition, a map,  $\mathcal{G}$ , is said to be diffeomorphic if  $\mathcal{G}$  and  $\mathcal{G}^{-1}$  are differentiable [26]. Bijectivity (i.e. one to oneness) and smoothness guarantee diffeomorphism. Therefore, by enforcing the map to be diffeomorphic, we ensure existence and uniqueness of  $\widetilde{\mathbf{M}}$ , given a  $\mathbf{M}$  and vice versa. Bijectivity is achieved by ensuring that volume of all the cells remain strictly positive. A negative cell volume leads to the indeterminate derivative of the state parameter, which can be seen as a ‘‘tear’’ in an image. Smoothness of the grid is maintained by penalizing abrupt changes of the grid volume, both in space and parameter/time. Any of the commonly used interpolation schemes between the constant grid and the learned grid can be utilized in this setting.

#### 3.2 Low-rank registration

So far, we only have tied the mapping to a time/parameter-varying grid, and have suggested that the mapping between the constant and the learned grid is simply an interpolation between them. In this section, the construction of the grid in the parameter/time space is discussed.

There are two general approaches to formulate the grid deformation in a registration problem. In the first class of approaches, the grid nodes are controlled as the solution of the a minimization problem. Diffeomorphism can then be achieved by enforcing a constraint on the determinant of the deformation

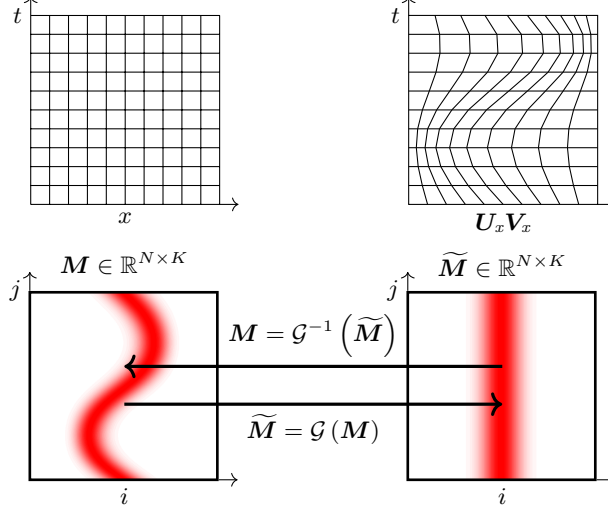


Figure 1: Illustration of proposed new nonlinear dimensionality reduction approach.

gradient: be strictly positive for all grid cells. This approach leads to a high-dimensional optimization problem which its nonlinearity and ill-posedness makes it computationally challenging [27]. In the second class of approaches, the mapping is the solution of a transport equation, i.e. flow fields, as in diffeomorphic dimensionality reduction [12]. Interestingly, in some special cases, a similar transport equation arises where the frame of references is changed from the Eulerian to the Lagrangian viewpoint, i.e. by solving the hyperbolic PDEs on the corresponding characteristic lines. This change of the reference is proven to be efficient in reduced order modeling of convection dominated PDEs [28, 29]. The existence of a low-rank near-optimal grid for many of the convection-dominated PDEs are demonstrated; However, the extension of this change of frame for any arbitrary systems is not straightforward. We leverage this premise in a data-driven setting. In our proposed method the coordinates of the grid at the  $n^{\text{th}}$  parameter or time-step is constructed as:

$$\mathbf{x}[n] := \mathbf{U}_x \mathbf{v}_{x_n}, \quad (4)$$

where  $\mathbf{v}_{x_n} \in \mathbb{R}^r$  is the  $n^{\text{th}}$  column of  $\mathbf{V}_x$  and  $\mathbf{U}_x \mathbf{V}_x$  is a rank- $r$  matrix,  $\mathbf{U}_x \in \mathbb{R}^{N \times r}$  and  $\mathbf{V}_x \in \mathbb{R}^{r \times K}$ , that represents the evolution of the parameter/time-varying grid, on which the low-dimensional latent variables lie. The rank- $r$  grid is then learned in (3). The latent variables can be interpreted as the evolution of the state parameters on the low-rank approximation of how the information travels, i.e. characteristic lines of the hyperbolic PDEs. This is one of the key elements of the proposed method, which greatly reduces the size of the optimization compared to existing registration-based methods, such as [21]. More importantly, it results in unprecedented predictive capabilities, i.e. accuracy beyond the training range.

### 3.3 Implementation

In this section, we summarize the elements of the proposed algorithm and make some clarifications on implementation of the method. As illustrated in Fig. 1, the procedure is designed to learn a low-rank grid,  $\mathbf{U}_x \mathbf{V}_x$ , on which the snapshot of the data,  $\widetilde{\mathbf{M}} = \mathcal{G}(\mathbf{M})$ , is low-rank. The final minimization problem has the following form:

$$\begin{aligned} & \underset{\mathbf{U}_x, \mathbf{V}_x}{\text{minimize}} && \left\| \mathbf{M} - \mathcal{G}^{-1}(\mathbf{U}\mathbf{V}) \right\|_F + \left\| \mathbf{\Gamma}_1 \mathbf{U}_x \right\|_F + \left\| \mathbf{V}_x \mathbf{\Gamma}_2^T \right\|_F, \\ & \text{subject to} && \mathbf{v}[n] \geq v_{\min}, \text{ for } n = 1, \dots, K, \\ & && \mathbf{x}[n]|_{\partial\Omega} = \mathbf{x}|_{\partial\Omega}, \text{ for } n = 1, \dots, K, \end{aligned} \quad (5)$$

where  $\mathbf{\Gamma}_1 \in \mathbb{R}^{N \times N}$  and  $\mathbf{\Gamma}_2 \in \mathbb{R}^{K \times K}$  are Tikhonov matrices designed to promote grid smoothness. Also  $\mathbf{v}[n] \in \mathbb{R}^{N-1}$  is a vector of cell volumes of the parameter/time-varying grid at the  $n^{\text{th}}$  parameter/time step,  $v_{\min}$  is the minimum admissible cell volume, and  $\mathbf{x}[n]|_{\partial\Omega}$  and  $\mathbf{x}|_{\partial\Omega}$  are boundary

points of the learned grid and the constant grid, respectively. The appropriate Tikhonov matrices and the minimum cell volumes are hyper-parameters and problem dependent.

Moreover, for practical reasons, a weak constraint on the rank reduction is chosen. While (3) implies minimizing over the rank of  $\widetilde{M}$ , in many cases, the solution of the minimization for a preset size of the decomposition is preferred. We assume  $\widetilde{M} = UV$ , where  $U \in \mathbb{R}^{N \times k_r}$ ,  $V \in \mathbb{R}^{k_r \times K}$ , and  $k_r \ll N$ ,  $k_r \ll K$ . Moreover, to reduce the size of the optimization problem,  $U_x$  and  $V_x$  are uniformly down-sampled, however, the objective is evaluated on the fine grid.

To interpolate the snapshots between the two sets of grid, we simply utilize a  $p$ -degree polynomial interpolation scheme. This choice innately incorporates a sparsity pattern into the mapping. While the latent space representation of a data-point on the learned grid using a nearest-neighbor interpolation only requires one data-point on the constant grid, a  $p$ -degree polynomial interpolation requires  $p - 1$  entries of the input vector. This, in principle, leads to a great reduction in the size the optimization problem compared to the traditional neural networks, where there is no *a priori* assumption on the structure of the connectivity between the nodes.

Finally, the proposed mapping can be utilized as an auto-encoder layer in a neural network (Fig. 2). This additional layer, greatly improves accuracy and training cost of neural network based models. The algorithm to train the proposed physics-aware registration based auto-encoder is summarized in Alg. 1.

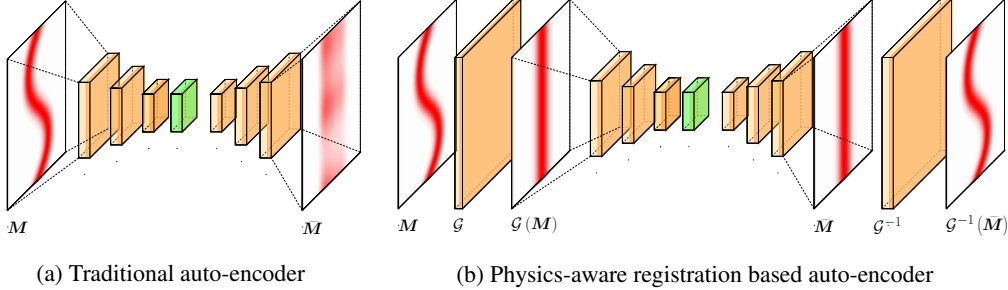


Figure 2: Network architecture to map the solution of a dynamical system onto a low-dimensional space and map it back to the high-dimensional space. The low-dimensional representation, the bottleneck, is depicted in green.

## 4 Experiments

We provide several experiments to demonstrate the superior capabilities of the proposed physics-aware registration based auto-encoder. In this section, we solve for the low-rank grid and test the reducibility/compression of the input as well as its application in a neural network architecture approximate the PDEs. We attempt to demonstrate both compression and interpretability of our results in these experiments. For all these experiments, we resort to readily available optimization packages capable of solving optimization with nonlinear constraints; such as `minimize` in `scipy` for our Python implementation, or `fmincon` in our Matlab implementation. Both of the implementations as well as the data and the results are made available at <https://github.com/rmojgani/PhysicsAwareAE>.

### 4.1 Manifold learning in rotated character ‘‘A’’

Consider a computer vision task of learning the nonlinear transformation, rotation, given a data-set comprised of a rotated character ‘‘A’’. The image of character ‘‘A’’ is stored in a  $50 \times 50$  matrix and is rotated a total of 90 degrees with 3 degrees increments resulting in a snapshot matrix of dimension  $2500 \times 31$ . A representative sample of the snapshots is shown in Fig. 3a, and a single POD mode reconstruction is illustrated in Fig. 3b. In this problem,  $U_x$  is down-sampled to size of 7, i.e. the total of 49 control points. Moreover,  $v_{\min} = 0$ ,  $\Gamma_1 = 100D_{xx}$  and  $\Gamma_2 = (100/\pi)D_{\theta\theta}$ , where  $D_{xx}$  and  $D_{\theta\theta}$  are the second derivative matrices in the spatial and parameter space, respectively. The

---

**Algorithm 1** Training the physics-aware registration based auto-encoder
 

---

**Input:** Hyper-parameters:  
 $\Gamma_1, \Gamma_2$ ,  
 Minimum admissible grid volume ( $v_{\min}$ ),  
 Reduction parameters:  
 Parameter/time-varying grid rank ( $r$ ),  
 Rank of the low-dimensional representation ( $k_r$ ),  
 The snapshots matrix ( $M \in \mathbb{R}^{N \times K}$ ),  
 Maximum number of iterations ( $j_{\max}$ ),

**Output:** Parameter/time-varying grid and its low-rank decomposition  $U_x V_x$ , such that  $x[n] := U_x v_{x_n}$ , and the corresponding maps, i.e.  $\mathcal{G}$  and  $\mathcal{G}^{-1}$

- 1: Initialize  $U_x \in \mathbb{R}^{N \times r}$  and  $V_x \in \mathbb{R}^{r \times K}$  with the SVD decomposition of the constant grid plus a small random perturbation
- 2:  $j \leftarrow 0$
- 3: **while**  $j \leq j_{\max}$  **do**
- 4:    $\widetilde{M} = \mathcal{G}(M)$  // Interpolate the snapshots onto  $U_x V_x$
- 5:    $UV \approx \widetilde{M}$  s.t.  $\text{rank}(UV) = k_r$  // Approximate  $\widetilde{M}$  using SVD as in (2)
- 6:    $\mathcal{G}^{-1}(UV)$  // Interpolate  $UV$  onto the constant grid
- 7:    $\|M - \mathcal{G}^{-1}(UV)\|_F + \|\Gamma_1 U_x\|_F + \|V_x \Gamma_2^T\|_F$  // Evaluate the objective
- 8:   Update  $U_x$  and  $V_x$  // Update the grid via the rule of the optimization
- 9:    $j \leftarrow j + 1$
- 10: **end while**

---

boundary point constraints are removed for this particular problem. The optimization problem of (5) approximates the rigid body rotation as in Fig. 3c. In Fig. 3d, the snapshots are approximated using a single basis ( $k_r = 1$ ) on the learned manifold of  $r = 2$ . The reconstruction delivered by the learned grid, using the proposed approach, is remarkably more accurate compared to the traditional POD approach.

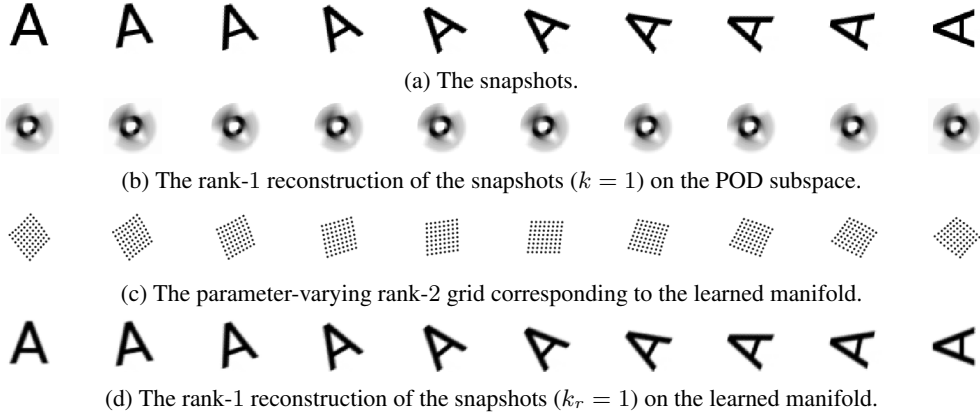


Figure 3: 90 degrees rotation of character “A”.

## 4.2 Manifold learning in two-dimensional fluid flows

In this section, the proposed manifold learning approach is applied to the two-dimensional Riemann problem of fluid dynamics,  $\frac{\partial}{\partial t} \mathbf{q} + \frac{\partial}{\partial x} \mathbf{f}_x + \frac{\partial}{\partial y} \mathbf{f}_y = 0$ , where  $\mathbf{q} = [\rho, \rho u, \rho v, \rho e]$ ,  $\mathbf{f}_x = [\rho u, \rho u^2 + p, \rho uv, \rho u H]$ ,  $\mathbf{f}_y = [\rho v, \rho v^2 + p, \rho v H]$ , and  $H = e + p/\rho$ ,  $p = \rho(\gamma - 1)(e - 0.5(u^2 + v^2))$  in the domain  $(x, y, t) \in [0, 1] \times [0, 1] \times [0, t_{\max}]$ , with initial conditions of configuration 3 and 12 as in [30]. The snapshots of primitive variables are generated using a high-order artificial viscosity scheme coupled with a 4<sup>th</sup>-order Runge-Kutta time discretization with  $\Delta t = 5 \times 10^{-4}$  on a  $150 \times 150$  grid. Snapshots are collected at  $\delta t = 0.016$  and  $\delta t = 0.006$  intervals for simulation range of  $t \in [0, 0.80]$  and  $t \in [0, 0.25]$  for configuration 3 and 12, respectively. The size of the snapshot matrices in both cases are  $10000 \times 50$ . A rank-2 time-varying grid ( $r = 2$ ) is learned via (5) setting

$k_r = 4$ , and  $\gamma_1 = \gamma_2 = 0.05$ , where  $\Gamma_1 = \gamma_1 \mathbf{D}_{xx} = \gamma_1 \mathbf{D}_{yy}$  is the second derivative matrix in the  $x$  and  $y$  directions and  $\Gamma_2 = \gamma_2 \mathbf{D}_{tt}$ , where  $\mathbf{D}_{tt}$  is the second derivative matrix in time. Also,  $v_{\min} = \Delta x_{\min} \Delta y_{\min}$ , where  $\Delta x_{\min} = \Delta y_{\min} = 6.7 \times 10^{-4}$ . The low-dimensional representation of density is compared on the constant grid and the learned manifold in Fig. 4. On the learned manifold, traveling shocks are conserved and free of non-physical oscillatory solutions, resulting in a significant error reduction.

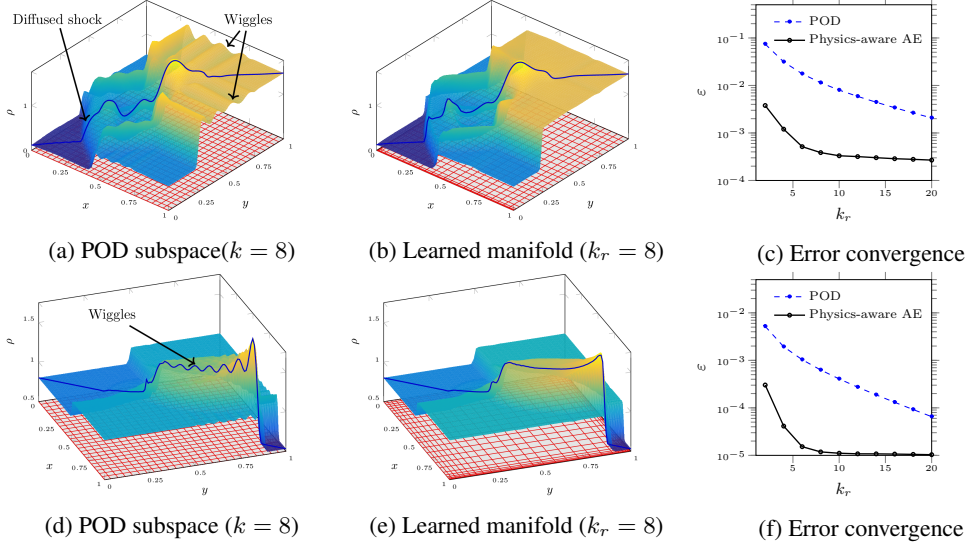


Figure 4: The density snapshots of the two-dimensional Riemann problems at the last time step of the simulations and the computational grid representative of the learned manifolds. Configuration 3: Fig. 4a to Fig. 4c; Configuration 12: Fig. 4d to Fig. 4f;

### 4.3 Physics based auto-encoder in an LSTM architecture

In this section, the proposed method is implemented as an auto-encoder layer wrapped around a traditional machine learning architecture to decrease the loss in compression phase and subsequently to improve the predictive capabilities of a recurrent neural network modeling the governing PDEs. We employ a long short-term memory (LSTM) to approximate the dynamics of the PDE on the learned manifold, a proven architecture to approximate PDEs [31]. To learn a low-dimensional manifold, a dense neural network with linear activation is used. Finally, the proposed registration based auto-encoder is added to the architecture.

Consider the scalar, one-dimensional nonlinear convection-diffusion equation, known as viscous Burgers' equation,  $\partial_t w(x, t) + w \partial_x w(x, t) = (1/Re) \partial_{xx} w(x, t)$  in the domain  $(x, t) \in [x_a, x_b] \times [0, T]$ , equipped with initial conditions  $w(x, 0) = w_0(x)$ , and Dirichlet boundary conditions at  $x_a$ , and  $x_b$ , where  $w(x, 0) = 0.8 + 0.5 e^{-(x-0.5)^2/0.1^2}$ ,  $w(x_a, t) = w(x_b, t) = 0$ , for  $(x, t) \in [0, 2.5] \times [0, 1]$ . An implicit second order time discretization is used with  $\Delta t = 8 \times 10^{-3}$  and space is uniformly discretized where  $\Delta x = 1 \times 10^{-2}$ . In the proposed architecture, the rank-1 time-varying grid ( $r = 1$ ), representing the physics-aware auto-encoder, is learned as in (5) with  $k_r = 4$ . In this problem,  $v_{\min} = 10^{-3}$ ,  $\Gamma_1 = \gamma_1 \mathbf{D}_{xx}$  and  $\Gamma_2 = \gamma_2 \mathbf{D}_{tt}$ , where  $\gamma_1 = \gamma_2 = 1$ , and  $\mathbf{D}_{xx}$  and  $\mathbf{D}_{tt}$  are second derivative matrices in space and time. Subsequently, the LSTM is trained to approximate  $\mathcal{G}(\mathbf{M})$ . In the traditional architecture, the densely connected auto-encoder and the LSTM are trained simultaneously (Fig. 2a). In the proposed architecture (Fig. 2b), the manifold and the neural network are trained separately. The neural network architectures are deployed in Keras [32]. The models are trained using the snapshot matrix of  $\mathbf{M} \in \mathbb{R}^{N_x \times N_t}$ . In the proposed physics-aware AE,  $\mathbf{V}_x$  is linearly extended. The contour plots of the solutions are compared in Fig. 5a and Fig. 5b. As expected, the neural network AE cannot predict the convection underlying the physics of the problem outside the training range (Fig. 5a); however, by leveraging the physics of the problem, the LSTM trained on the low-dimensional manifold realized by the registration-based AE leads to a solution much closer to the solution of the PDE (Fig. 5b). The mean squared difference of the solutions,  $\epsilon$ , for different sizes of LSTM,  $N_h$ , are plotted in Fig. 5c.

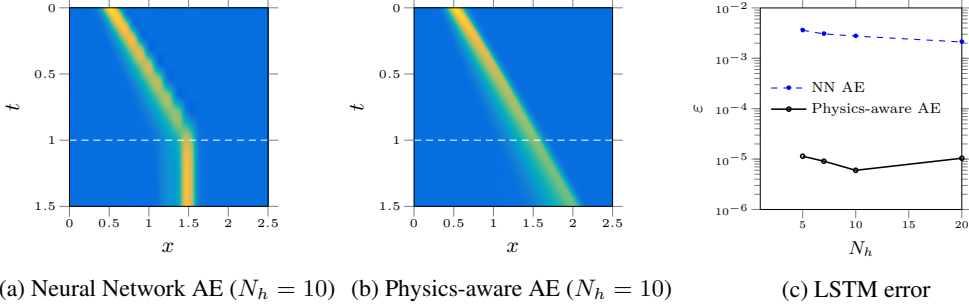


Figure 5: LSTM approximating the Burgers' equation.

Also, consider the one-dimensional wave equation,  $\partial_{tt}w(x, t) - \partial_{xx}w(x, t) = 0$ , in the domain  $(x, t) \in [x_a, x_b] \times [0, T]$ , equipped with initial conditions  $w(x, 0) = w_0(x)$ , and Dirichlet boundary conditions at  $x_a$ , and  $x_b$ , where  $w(x, 0) = e^{-(x-0.5)^2/0.1^2}$ ,  $w(x_a, t) = w(x_b, t) = 0$ , for  $(x, t) \in [0, 1] \times [0, 1]$ . An implicit second-order time-discretization is used with  $\Delta t = 2.5 \times 10^{-3}$  and space is uniformly discretized where  $\Delta x = 10^{-2}$ . The architecture is set up similar to the Burgers' equation, with the following parameters: the time-varying grid is of rank-2 ( $r = 2$ ), the reconstruction on the learned manifold is of rank-2 ( $k_r = 2$ ),  $v_{\min} = 10^{-3}$ ,  $\gamma_1 = \gamma_2 = 10$ , and the size of the grid bases, in both space and time, are down-sampled to 15 control points. The solution and error are plotted in Fig. 6, showing the performance of the proposed physics-aware AE compared to the traditional architecture.

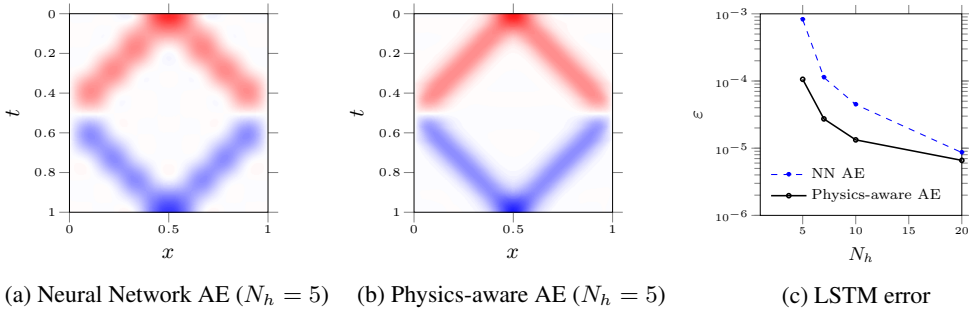


Figure 6: LSTM approximating the wave equation.

## 5 Conclusion

We have proposed a variation to the diffeomorphic [12] or the registration based [21] manifold learning methods for dimensionality reduction of convection dominated PDEs, where the Kolmogorov n-width of the snapshots is large. The existence of a low-rank parameter/time-varying grid [28, 29], is leveraged to decrease the Kolmogorov n-width of such problems in a data-driven settings. In the proposed registration, the solution of the PDEs is mapped onto a non-uniform parameter/time-varying grid, such that the Kolmogorov n-width of the latent snapshots is minimized. This is achieved using a low-rank linear decomposition of the snapshots on the learned grid, a relatively low-cost computation compared to training of any of the existing nonlinear manifold learning approaches. We have demonstrated the application of the proposed physics-aware auto-encoder on a computer vision task, an image under nonlinear transformation, and solution of nonlinear convection dominated PDEs, two-dimensional Riemann problem and Burgers' equation. Leveraging the low-rank structure of the grid has enabled us with an interpretable map that can be manipulated to fit the underlying convection in the problem. We have incorporated the dimensionality reduction as an auto-encoder layer in training of recurrent neural networks reproducing PDEs. Moreover, we have shown it outperforms a neural network-based auto-encoder in prediction of the system beyond the training range. The proposed approach has the potential to be generalized to PDEs of higher spatial dimensions, as well as to greatly decrease the size of more traditional projection-based model order reduction techniques.

More importantly, it shows the potential to lower the training costs and enhance the predictive capabilities of models learned in system identification settings.

## References

- [1] Ariana Mendible, Aleksander Aravkin, Wes Lowrie, Steven Brunton, and J. Nathan Kutz. Dimensionality reduction and reduced order modeling for traveling wave physics. *arXiv preprint arXiv:1911.00565v1*, 2019.
- [2] Geoffrey E Hinton, Michael Revow, and Peter Dayan. Recognizing handwritten digits using mixtures of linear models. In G. Tesauro, D. S. Touretzky, and T. K. Leen, editors, *Advances in Neural Information Processing Systems 7*, pages 1015–1022. MIT Press, 1995.
- [3] Michael A. A. Cox and Trevor F. Cox. Multidimensional scaling. In *Handbook of Data Visualization*, pages 315–347. Springer Berlin Heidelberg, Berlin, Heidelberg, 2008.
- [4] Jerome Friedman, Trevor Hastie, and Robert Tibshirani. *The elements of statistical learning*. Number 10 in 1. Springer series in statistics New York, 2001.
- [5] Joshua B. Tenenbaum. Mapping a manifold of perceptual observations. In M. I. Jordan, M. J. Kearns, and S. A. Solla, editors, *Advances in Neural Information Processing Systems 10*, pages 682–688. MIT Press, 1998.
- [6] Sebastian Mika, Bernhard Schölkopf, Alex J. Smola, Klaus-Robert Müller, Matthias Scholz, and Gunnar Rätsch. Kernel pca and de-noising in feature spaces. In M. J. Kearns, S. A. Solla, and D. A. Cohn, editors, *Advances in Neural Information Processing Systems 11*, pages 536–542. MIT Press, 1999.
- [7] S. T. Roweis. Nonlinear dimensionality reduction by locally linear embedding. *Science*, 290(5500): 2323–2326, December 2000. ISSN 00368075.
- [8] Mikhail Belkin and Partha Niyogi. Laplacian eigenmaps for dimensionality reduction and data representation. *Neural Computation*, 15(6):1373–1396, jun 2003. ISSN 0899-7667.
- [9] Kilian Q. Weinberger, Fei Sha, and Lawrence K. Saul. Learning a kernel matrix for nonlinear dimensionality reduction. In *Twenty-first international conference on Machine learning - ICML '04*, page 106, New York, New York, USA, 2004. ACM Press. ISBN 1581138285.
- [10] Hinton G.E and Salakhutdinov R.R. Reducing the dimensionality of data with neural networks. *Science*, 313(July):504–507, 2006. ISSN 0036-8075.
- [11] Laurens van der Maaten and Geoffrey Hinton. Visualizing data using t-SNE. *Journal of machine learning research*, 9(November):2579–2605, 2008.
- [12] Christian Walder and Bernhard Schölkopf. Diffeomorphic dimensionality reduction. In D. Koller, D. Schuurmans, Y. Bengio, and L. Bottou, editors, *Advances in Neural Information Processing Systems 21*, pages 1713–1720. Curran Associates, Inc., 2009.
- [13] Kookjin Lee and Kevin T Carlberg. Model reduction of dynamical systems on nonlinear manifolds using deep convolutional autoencoders. *Journal of Computational Physics*, 404:108973, March 2020. ISSN 00219991.
- [14] Jonathan Masci, Ueli Meier, Dan Cireşan, and Jürgen Schmidhuber. Stacked convolutional auto-encoders for hierarchical feature extraction. In *International conference on artificial neural networks*, pages 52–59. Springer, 2011.
- [15] Alec Radford, Luke Metz, and Soumith Chintala. Unsupervised representation learning with deep convolutional generative adversarial networks. *CoRR*, abs/1511.06434, 2015.
- [16] M. Cheng, F. Fang, C.C. Pain, and I.M. Navon. Data-driven modelling of nonlinear spatio-temporal fluid flows using a deep convolutional generative adversarial network. *Computer Methods in Applied Mechanics and Engineering*, 365:113000, June 2020. ISSN 00457825.
- [17] Bernd R. Noack, Marek Morzynski, and Gilead Tadmor. *Reduced-order modelling for flow control*, volume 528 of *CISM International Centre for Mechanical Sciences*. Springer Science & Business Media, 2011.
- [18] Philip Holmes, John L. Lumley, Gal Berkooz, and Clarence W. Rowley. *Turbulence, coherent structures, dynamical systems and symmetry*. Cambridge University Press, 2nd edition, 2012.

- [19] J Nathan Kutz, Steven L Brunton, Bingni W Brunton, and Joshua L Proctor. *Dynamic mode decomposition: data-driven modeling of complex systems*. SIAM, 2016.
- [20] Craig Gin, Bethany Lusch, Steven L Brunton, and J Nathan Kutz. Deep learning models for global coordinate transformations that linearize pdes. *arXiv preprint arXiv:1911.02710*, 2019.
- [21] Tommaso Taddei. A registration method for model order reduction: Data compression and geometry reduction. *SIAM Journal on Scientific Computing*, 42(2):A997–A1027, January 2020. ISSN 1064-8275.
- [22] Seddik M. Djouadi. On the connection between balanced proper orthogonal decomposition, balanced truncation, and metric complexity theory for infinite dimensional systems. *Proceedings of the 2010 American Control Conference, ACC 2010*, pages 4911–4916, 2010.
- [23] Lawrence Sirovich. Turbulence and the dynamics of coherent structures. part I: Coherent structures. *Quarterly of Applied Mathematics*, 45(3):561–571, 1987.
- [24] Colin Fyfe. A neural network for pca and beyond. *Neural Processing Letters*, 6(1-2):33–41, 1997.
- [25] Michael P. Holmes, Alexander G. Gray, and Charles Lee Isbell. QUIC-SVD: Fast SVD using cosine trees. *Advances in Neural Information Processing Systems 21 - Proceedings of the 2008 Conference*, pages 673–680, 2009.
- [26] Jan Modersitzki. *FAIR: Flexible Algorithms for Image Registration*. Society for Industrial and Applied Mathematics., 2009.
- [27] Andreas Mang, Amir Gholami, Christos Davatzikos, and George Biros. PDE-constrained optimization in medical image analysis. *Optimization and Engineering*, 19(3):765–812, September 2018. ISSN 1389-4420.
- [28] Rambod Mojjani and Maciej Balajewicz. Lagrangian basis method for dimensionality reduction of convection dominated nonlinear flows. *arXiv preprint arXiv:1701.04343*, 2017.
- [29] Hannah Lu and Daniel M. Tartakovsky. Lagrangian dynamic mode decomposition for construction of reduced-order models of advection-dominated phenomena. *Journal of Computational Physics*, 407:109229, April 2020.
- [30] Peter D. Lax and Xu-dong Liu. Solution of two-dimensional Riemann problems of gas dynamics by positive schemes. *SIAM Journal on Scientific Computing*, 19(2):319–340, March 1998.
- [31] Eric J. Parish and Kevin T. Carlberg. Time-series machine-learning error models for approximate solutions to parameterized dynamical systems. *Computer Methods in Applied Mechanics and Engineering*, 365:112990, June 2020. ISSN 00457825.
- [32] François Chollet et al. Keras. <https://keras.io>, 2015.